Dicle University Journal of Engineering (DUJE)

web: http://dergipark.gov.tr/dumf

Research Article

Spatial variation model of seismic ground motion for Istanbul

Ebru Harmandar [1,*], Eser Çaktı[2], Mustafa Erdik[2]

[1] Department of Civil Engineering, Faculty of Engineering, Muğla Sıtkı Koçman University, Muğla, Turkey; ORCID ID: 0000-0001-9802-2993

[2] Department of Earthquake Engineering, Boğaziçi University, Kandilli Observatory and Research Institute, İstanbul, Turkey

ARTICLE INFO

Article history:

Received 16 March 2020
Received in revised form 5 October 2020
Accepted 7 October 2020
Available online 13 January 2021

Keywords:

Istanbul Earthquake Rapid Response System, Coherency Model, Target Spectrum, Spectral Matching, Spatially Variable Simulated Earthquake Data

Doi: 10.24012/dumf.701211

ABSTRACT

Earthquake induced base motions of elongated structures will not be uniform. This variation of ground motion has a nonnegligible effect on the dynamic response of lifelines that has led to investigations of characterization and modelling of the spatially varying earthquake ground motion within the last decade. In this context, spatial variation of seismic ground motion in Istanbul is analyzed. After the introduction of the concept of coherency function and its conventional estimation procedure, estimation of coherency from recorded data and its interpretation are presented. The lagged coherency is calculated by the conventional coherency estimation scheme applied to six earthquakes registered by the Istanbul Earthquake Rapid Response System. A coherency model for Istanbul is derived that will enable to simulate spatially variable ground motion needed as input in the design of extended structures. Simulation of ground motion at pairs of closely spaced locations is presented that consider the derived coherencies in their scheme. The results are compared with actual recordings from the same locations. Simulation of spatially variable ground motion consistent with a coherency function is stated.

* Corresponding author
Ebru Harmandar
✉ e-mail: ebruharmandar@mu.edu.tr

Please cite this article in press as E. Harmandar, E. Çaktı, M. Erdik, "Spatial variation model of seismic ground motion for Istanbul", DUJE, vol. 12, no.1, pp. 111-131, January 2021.

Introduction

Several researches have been done about the relationship between coherency, frequency of earthquake ground motion, and the distance among the stations. For the quantification of the variability of seismic ground motion, Fourier amplitude spectra is used by Schneider et al. [1]; acceleration response spectra is studied by Abrahamson and Sykora [2]; the correlation between the peak ground acceleration (PGA), peak ground velocity (PGV) and magnitude, distance and site conditions is examined by Joyner and Boore [3] and Abrahamson [4]. The variability of PGAs as a function of separation distance among the stations is studied by Kawakami and Mogi [5]. Additionally, Field et al. [6] examined the pseudo-velocity response spectra (PSV) in terms of variability. The analyses repeated for the relation between the PSV and inter-station distance by Evans et al. [7]. Moreover, the spatial variation is described by coherency. The strong dependence of spatial variation of strong ground motion on frequency has been indicated in early studies by Loh [8], McLaughlin [9], Abrahamson [10] among others. Coherency models have been developed by several researchers such as Abrahamson [11], Harichandran and Vanmarcke [12], Harichandran [13], Harichandran [14], Loh [8], Loh and Yeh [15], Loh and Lin [16], Novak [17], Oliveira et al. [18], Ramadan and Novak [19], Vernon et al. [20], Zerva and Zhang [21], and Cacciola and Deodatis [22]. An overview of the spatial variation of ground motion has been done by Zerva and Zervas [23] and Zerva [24]. Song et al. [25] explored the relation between spatial coherence between earthquake source parameters. The statistical properties of spatial variability of ground motion data of two earthquakes recorded by IERRS have been studied by Harmandar et al. [26, 27]. A new methodology has been developed for the interpolation of peak ground acceleration (PGA) from discrete array stations using data from IERRS by Harmandar et al. [28].

Consideration of spatial variability in modelling of earthquake ground motion is important for the design of above or under ground structures and systems where multiple-support excitation needs to be considered. Spectral representation method [29, 30]; auto-regressive, moving-average, and auto-regressive-moving-average models [31, 32, 33, 34]; local average subdivision method [35] and the covariance matrix decomposition [36, 37] are some of the methods used for the simulation of spatially variable strong ground motion. Additionally, Abrahamson [38] studied envelope functions considering random phase variability; Ramadan and Novak [39] proposed coherency function estimation using a Fourier series. Moreover, Yamamoto [40] proposed that for the probabilistic assessment of the performance of structures ground motion simulation with appropriate coherency is required.

As aforementioned, uniform earthquake ground motion data cannot reflect the spatial variability of field. For stochastic response analysis and reliability assessment of extended and multi-supported structures, coherence model is necessary for this variability effect. Besides, several bridges and infrastructures have been built in Istanbul. For the design of these extended structures, it is important to investigate the spatial variability of earthquake ground motion data.

In this context, the purpose of this study is to derive a coherency model, which could be used in the simulation of non-stationary ground motion needed for the design of extended structures, based on data recorded by Istanbul Earthquake Rapid Response System (IERRS) stations. Istanbul is the most important city in the world that has suffered many devastating earthquakes throughout history, such as the 1766 Istanbul earthquake with an estimated magnitude of 7.1. Therefore, it is crucial to handle the properties of earthquake data, which affect the dynamic analysis of extended structures.

Furthermore, simulation of ground motion compatible with target spectrum is constituted using the computed coherency model. The aim is to simulate earthquake ground motion data for the absent stations throughout in an array, considering a reference station.

Determination of coherency

The procedure for analyzing stochastic spatial variation of seismic motions from recorded data is considered to be realizations of random space-time fields. To obtain the information about spatial variability, some assumptions should be

done: The random field is homogeneous in space; the time histories recorded at stations are stationary random processes; stationary time histories at the recording stations are ergodic. For the characterization of random field, the definition of coherency is required in terms of cross spectral density and power spectral density.

Definition of coherency

The cross spectrum of the time histories can describe the random field of data as

$$S_{xy}(w) = \sum_{m=-M}^{+M} W(m\Delta w) A_x^*(w + m\Delta w) A_y(w + m\Delta w) \quad (1)$$

where M is the spectral window, $W(w)$, is the Fourier transform of lag window, $\Delta w$is the frequency step, A is Fourier transform of time histories, *m* is , and * is complex conjugate.

The power spectrum of data at two stations on ground surface is expressed as

$$S_{xy}(w) = \sum_{m=-M}^{+M} W(m\Delta w) \left| A_k(w + m\Delta w) \right|^2 \quad (2)$$

Correlation and coherency can characterize the spatial variability of ground motion. Correlation represents the phase variability in time; coherency represents in frequency domain. The coherency is used due to its mathematical relevance in random vibration analysis. The variability in frequency domain is studied by Matsushima [42], Abrahamson [43], Harichandran [14], and Zerva and Zervas [23]. The coherency function $\gamma_{xy}(\omega)$, between ground motion data at two stations x and y is given as :

$$g_{xy}(w) = \frac{S_{xy}(w)}{\sqrt{S_{xx}(w) S_{yy}(w)}} \quad (3)$$

in which ω is frequency, $S_{xy}(\omega)$ is the cross-power spectral density between stations x and y, $S_{xx}(\omega)$ is the power spectral density at station x and $S_{yy}(\omega)$ is the power spectral density at station y. The results of coherency will be complex numbers. When the absolute value of the coherency (lagged coherency) is taken, the effects of inclined plane wave propagation will be removed. It is generally used in engineering purposes [44].

Array configuration and earthquakes

The Earthquake Rapid Response System in Istanbul (IERRS) is composed of 100 strong motion stations and associated peripherals for data storage and communication. A significant number of earthquake events are registered by the IERRS six of which are utilized in this study for the estimation of coherency values. A comprehensive description of the IERRS can be found in Erdik et al. [45]. Figure 1 provides the distribution of 100 IERRS stations. Harmandar et al. [28] represented that the station separation distances of the IERRS vary from 0.67 km to 56 km. The epicenters of earthquakes utilized in the present work are shown in Figure 2. General properties of the chosen events are summarized in Table 1.

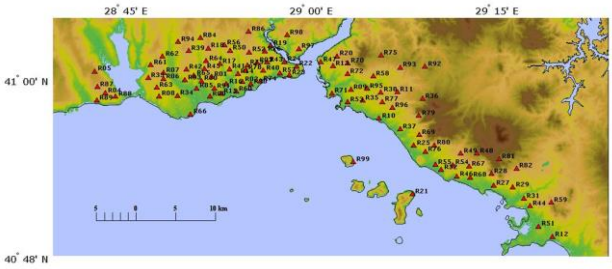

Figure 1. Locations of the stations in Istanbul Earthquake Rapid Response System (Harmandar et al. [28])

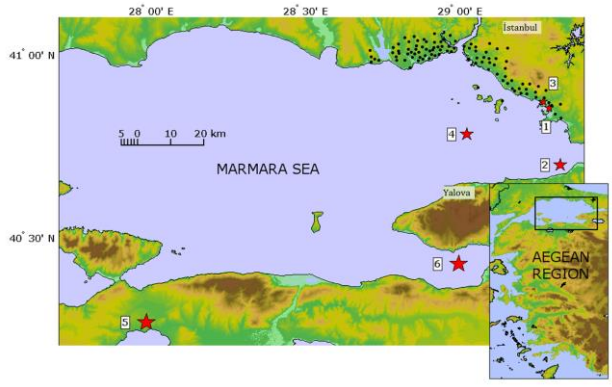

Figure 2. Epicenters of the selected earthquakes recorded by the Istanbul Earthquake Rapid Response System (after Harmandar et al. [28])

Data processing

For the generation of the coherency values, selection of the specific time windows is

necessary. The shear wave part of acceleration in most cases has the strongest energy in the record, and generally, is the most damaging component from the engineering perspective.

The baseline-corrected acceleration traces are filtered with a butter-worth filter (4^{th} order) using the range detected by Fourier amplitude spectrum and signal to noise ratio. The selected time windows are aligned by considering a reference station to remove the apparent wave propagation effect across the array for a better characterization of the homogeneity of ground motion [46]. Also, high frequency surface waves and the variation of the low frequency surface waves generated by wave propagation in the crust are not observed over the shallow depth range in the area [47]. S-wave window lengths are identified and a five per cent cosine tapering is applied. After preprocessing and alignment operations, the coherency function is obtained by estimating the power spectral densities and cross-spectral density (Figure 3).

Evaluation of coherency values

Application of smoothing windows is essential in the coherency spectrum estimation procedure. An 11-point Hamming window is suggested when the data length is less than 2000 steps and the coherency estimates are intended for structural analysis [44].

A code is written in MATLAB environment for the calculation of the coherency values. Its flowchart is shown in Figure 3. Data taken from Event 5 triggered by the SMART-1 array [48] are used for the application of the code. The calculated coherencies based on SMART-1 data for a window length of 5 are illustrated in Figure 4.

After the application of the code, the coherency values for the six events recorded by IERRS are calculated for the different station separation distance bins. Earthquake ground motion data from east-west (EW); north-south (NS); radial (R); and transversal (T) components are used in the analyses. Two different windows are considered: 11- and 15- point hamming windows. Seven distance bins are used. The bins are represented in Figure 5. The average values of coherencies are used in each distance bin. In Figure 5, the average coherency values are shown for the September 29, 2004 earthquake. For all remaining events studied, not shown here for brevity, the coherencies of EW component of the data using 11-point hamming window show more coherent distribution with distance and frequency than the others. As shown in Figure 5, coherency values calculated from EW component using 11-point hamming window are higher than the coherencies of NS, R and T components for both 11- and 15-point window lengths. Coherence values are predicted to decrease as separation distance increases. EW component has higher coherency at about 3 Hz for the separation distance 0-2 km (Fig. 5a). Also, the behaviour of EW coherency with respect to frequency is clearer. As a result, for the estimation of the coherency values, the window length is selected as 11 point based on Abrahamson et al. [44] suggestions. Finally, R and T components of coherency values are considered to examine the relationship between wave propagation and the coherency. There was no compatibility between coherency and wave propagation direction for earthquake ground motion data triggered by six earthquakes. Each station pair has a different separation distance. The distributed distances should be categorized due to an accurate regression analysis.

The coherency values for distance bins associated with September, 19 2003; May 16, 2004; September, 29 2004; October 20, 2006; October 24, 2006; and March 12, 2008 earthquakes are demonstrated by Figure 6; (a), (b), (c), (d), (e), and (f), respectively. 332 ground motion data are used, totally. 9837 sets are utilized to obtain the coherency values in Eq. 1. As shown in Figure 6, coherency values for frequency-distance behaviour is not clear in terms of dependence of magnitude. The main reason behind this is that the number of recording stations and their location vary from earthquake to earthquake. For example for the earthquake in Figure 6a, although the epicentral distances were smallest, the number of recording stations was relatively small. Therefore, the coherency behaviour is not explicit. In Figure 6b and Figure 6c, the coherency values in terms of distance and frequency is clearly presented. The reason is attributed to higher number of earthquake ground motion data in these two earthquakes. High coherencies (0.8) are detected in the distance range of 1.5-3 km for frequencies

of 0-3 Hz except for September 19, 2003 (Figure 6a) and November 20, 2006 earthquakes (Figure 6b). Mostly, coherency values are higher than 0.6 at the frequencies less than 5 Hz. Coherency values are approximately 0.65 at the frequencies 2-4 Hz and at the distances 1.5-2.8 km (Figure 6b, c, e, f).

Process for coherency model

As it is known and estimates based on IERRS data, the decay of the coherency in terms of frequency and distance is approximately exponential (Figure 5).

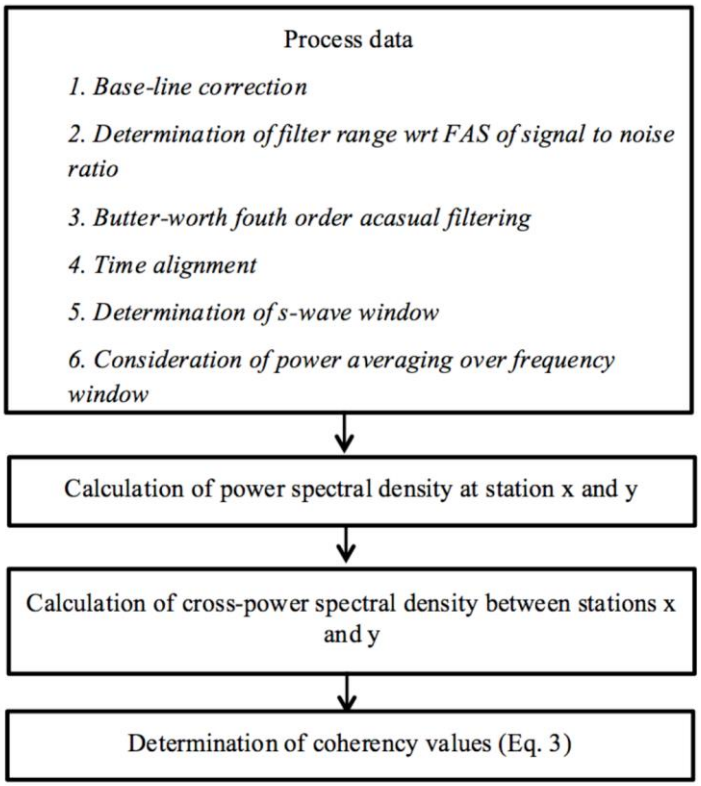

Figure 3. Procedure for calculation of coherency values

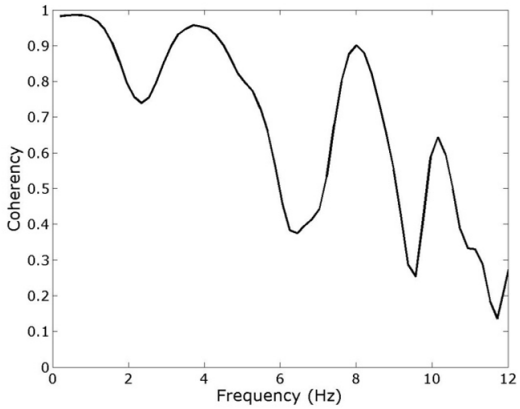

Figure 4. The lagged coherency between stations I06 and I12 recorded by SMART-1 (Window length, M =5)

Table 1. Source properties of the earthquakes registered by IERRS (http://www.koeri.boun.edu.tr/sismo/default.htm) (after Harmandar et al. [28])

Eq No	Earthquake	Date	Latitude N	Longitude E	GMT	M_L	M_d	Depth (km)	Fault mechanism	Number of recording stations	Maximum Epicentral Distance (km)	Minimum Epicentral Distance (km)
1	Güzelyalı	19/09/2003	40.8498	29.2867	00:51	3.1	3.2	10.3	Strike-slip	16	16	1
2	Yalova	16/05/2004	40.6957	29.3222	03:30	4.3	4.2	9.1	Strike-slip	72	58	14
3	Marmara Sea	29/09/2004	40.7797	29.0200	15:42	4.0	-	8.3	Strike-slip	86	34	14
4	Kuşgölü	20/10/2006	40.2635	27.9843	21:15	-	5.2	5.4	Strike-slip	43	130	101
5	Gemlik	24/10/2006	40.4240	28.9947	17:00	-	5.2	9.2	Strike-slip	47	70	52
6	Çınarcık	12/03/2008	40.6210	29.0110	20:52	4.8	-	8.9	Normal	54	50	30

M_d : Earthquake Duration Magnitude, M_L : Local Magnitude

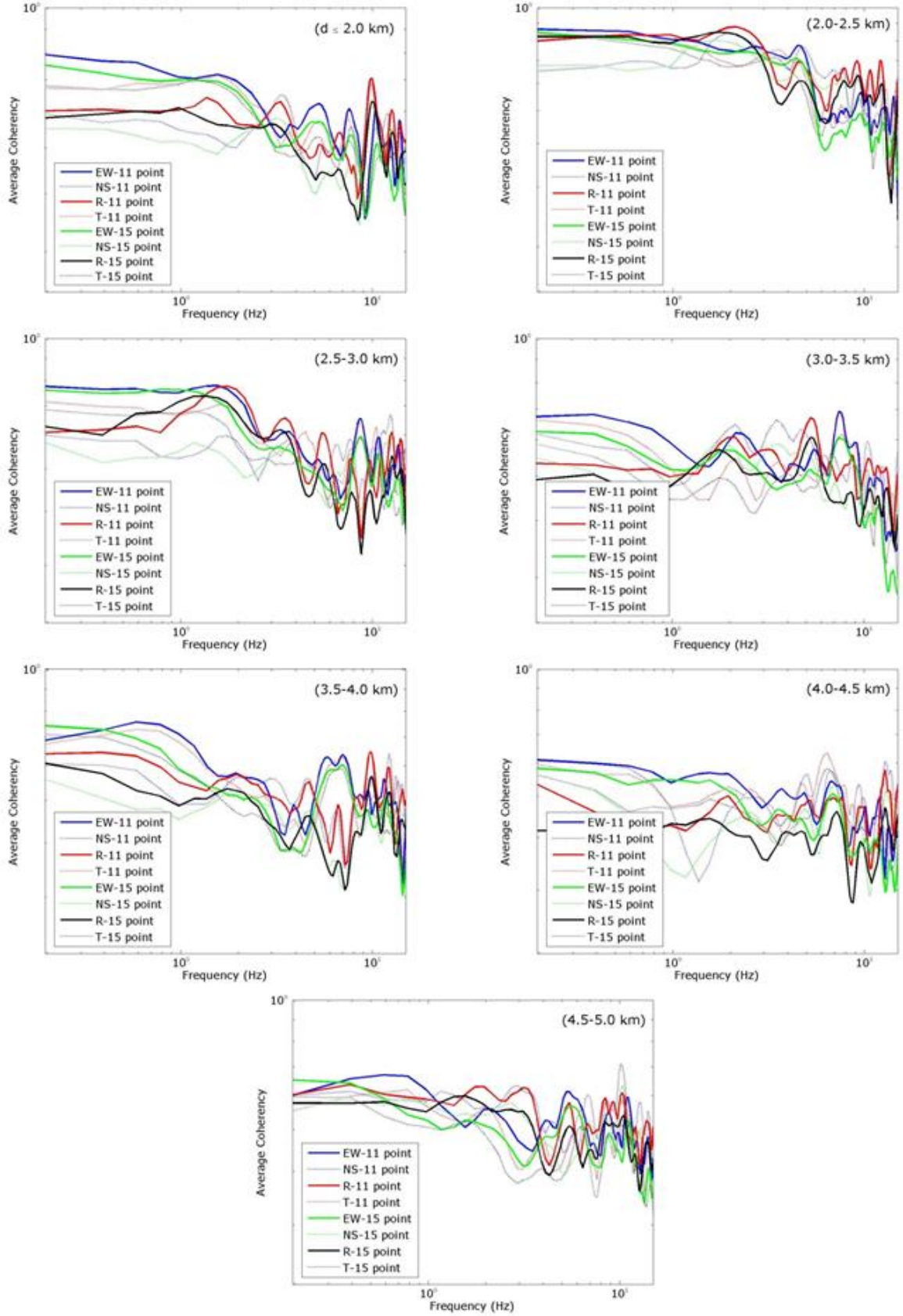

Figure 5. Average coherency values of distance bins with respect to direction and smoothing window length –September 29, 2004 earthquake

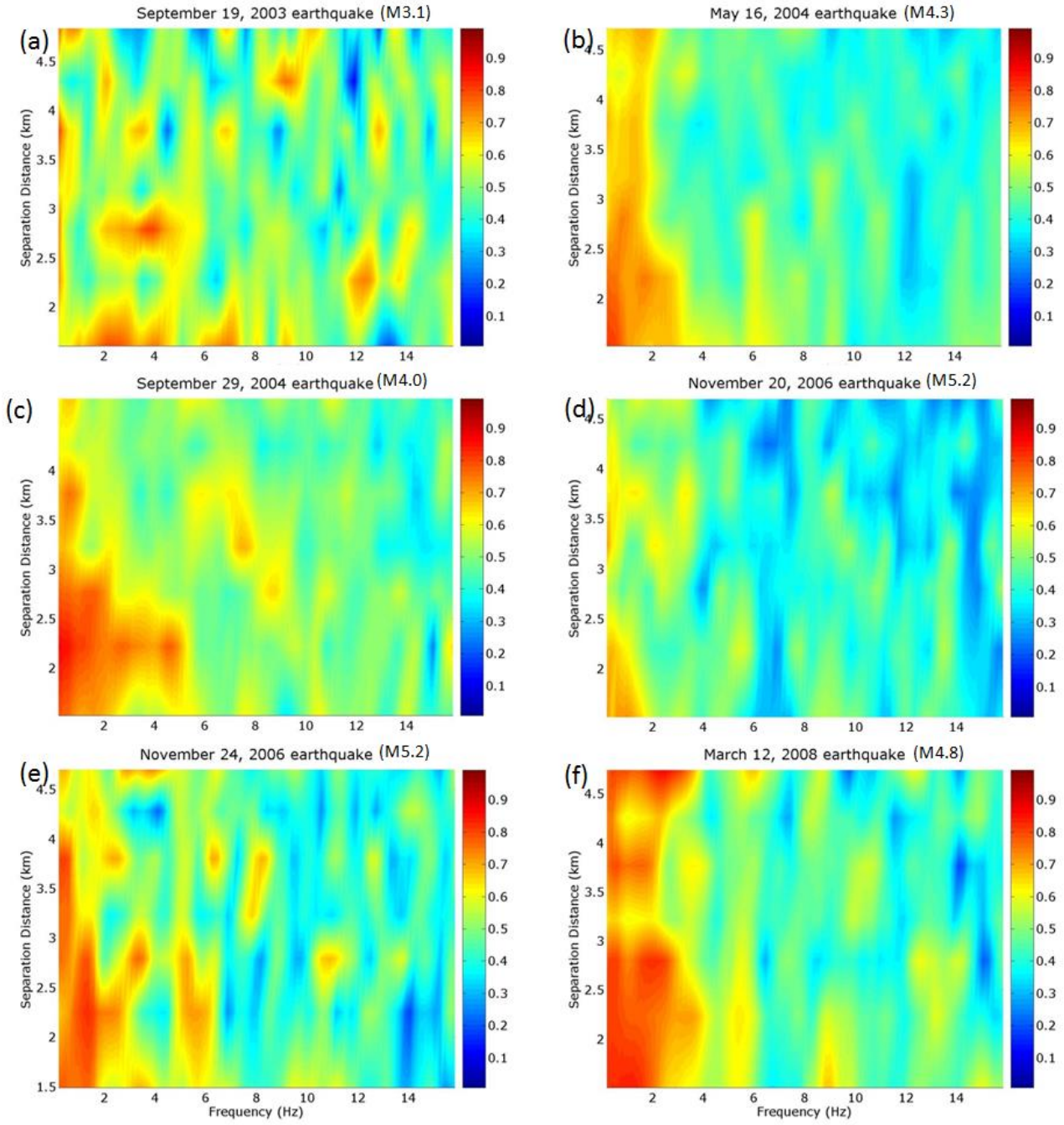

Figure 6. Coherency values for distance ranges in the EW direction (11-point): (a) September, 19 2003 earthquake; (b) May 16, 2004 earthquake; (c) September, 29 2004 earthquake, (d) October 20, 2006 earthquake, (e) October 24, 2006 earthquake, (f) March 12, 2008 earthquake

Based on the aforementioned proposed models in the literature, this exponential decay and variation of frequency and distance decay, the coefficients are situated. Therefore, the following initial coherency model is selected:

$$|\gamma(d,f)| = a_1 + e^{-(a_2 \times d)^2} + e^{-(a_3 \times f)^2} \quad (4)$$

where γ is the coherency; a_1, a_2, and a_3 are constants; d is the station separation distance; f is the frequency. The least-squares regression of the coherency on frequency by distance bins yields parameters a_1, a_2, and a_3. As this initial model (Eq. 4) did not match all data and earthquakes, particularly due to misfits associated with distance, it is improved as in Eq. 5:

$$|\gamma(d,f)| = a_1 + \left(\frac{a_2}{d}\right)\left(e^{-(d)^2} + e^{-(a_3 \cdot f)^2}\right) \quad (5)$$

In this formula, the parameter a_3, which is related to distance, does not converge due to the irregularities of coherency values with respect to distance (Table 2). When the separation distance is taken as zero or almost zero, the coherency should be one or close to one. Eq. 5 has the inverse separation distance as a variable that forces it to infinity when the separation distance is zero. Therefore a new equation related to Eq. 5 needs to be developed, where both the frequency and distance variables are in exponential terms. The equation is expressed as

$$|\gamma(d,f)| = a_1 e^{(a_2 - a_3\sqrt{d})0.01f} + (1 - a_1) e^{(-a_4 - a_5 d^2)(0.01f)^2} \quad (6)$$

Again, regression analyses to obtain coherency model are proposed by considering six earthquakes individually. Table 3 summarizes the results of regression analysis. The last column of Table 3 shows the results of the regression analysis carried out using the whole data set. It is seen that five regression parameters, a_1, a_2, a_3, a_4, and a_5, are close to each other for every earthquake and the whole earthquake dataset. Figure 7 represents the comparison of the coherency model with respect to observed coherency values for distance bins d=2.0-2.5 km and d=4.5-5.0 km.

The difference of observed and estimated coherency values are logarithmically calculated to obtain the residuals. In Figure 8, the logarithmic residuals of these six earthquakes are shown for seven separation distance bins. All residuals involve the combination of coherency values calculated from the six earthquakes. The mean residuals range from +0.2 to -0.2. As it seems in Figure 8, residuals do not have any systematic trend and dependency on the frequency or the distance bin.

The coherency model, calculated by Eq. 6 using data from earthquakes having magnitudes smaller than 5.2, for Istanbul is shown in Figure 9 for different distances: 100m, 300m, 500m, 1000m, 3000m, and 5000m.

Simulation of spatially variable ground motion

Methodology

In addition to realistic characterization of spatial variation, simulation of spatially varying time histories is a crucial part of the study considering the structural response of extended structures [49]. However, the generation of spatially variable ground motion for the performance-based design of lifeline structures, such as bridges, dams, pipelines, power transmission systems, etc., will be received the attention it deserves [50]. Das and Gupta [51], Bi and Hao [52], Abrahamson [38] and Abrahamson [11] proposed methods for generating spatially variable ground motion given a target spectrum, coherency function and an initial time history. An approach is developed by Shama (2007) for the simulation of spatially correlated ground motion at different stations with respect to a reference record subdivided into time windows for the treatment of frequency and temporal variations. Simulated ground motion is compatible with the target auto spectrum of the reference record and the coherency function. According to Shama [34], this method is accurate to generate spatially correlated ground motion for multi-supported structures.

The estimated data should be consistent with the defined target spectrum at a reference station and the coherency values of these estimated data have to be compatible with

Table 2. Regression coefficients based on Eq. 5 for East-West direction of the earthquakes data recorded by IERRS

	2003.09.19 earthquake	2004.05.16 earthquake	2004.09.29 earthquake	2006.10.20 earthquake	2006.10.24 earthquake	2008.03.12 earthquake	All data
a_1	0.4369	0.4238	0.4762	0.3846	0.4298	0.4551	0.440
a_2	0.3951	0.6719	0.5082	0.5497	0.5888	0.062	0.564
a_3	508.6517	17.4640	-43.7637	-1.2550	2177.3574	108.9232	35.239
a_4	0.0999	0.2577	0.1899	0.2887	0.1845	0.2569	0.214

Table 3. Regression coefficients based on Eq. 7 for data recorded by IERRS

	2003.09.19 earthquake	2004.05.16 earthquake	2004.09.29 earthquake	2006.10.20 earthquake	2006.10.24 earthquake	2008.03.12 earthquake	All data
a_1	0.5298	0.4813	0.5620	0.4708	0.4702	0.5023	0.5130
a_2	0.0253	0.0867	0.4155	0.0777	0.1071	0.1320	0.0781
a_3	0.0170	0.0399	0.0263	0.0446	0.0398	0.0517	0.0380
a_4	0.3795	0.1925	0.1444	0.3081	0.2137	0.1926	0.2643
a_5	0.0067	0.0233	0.0409	0.1000	0.0248	0.0302	0.0301

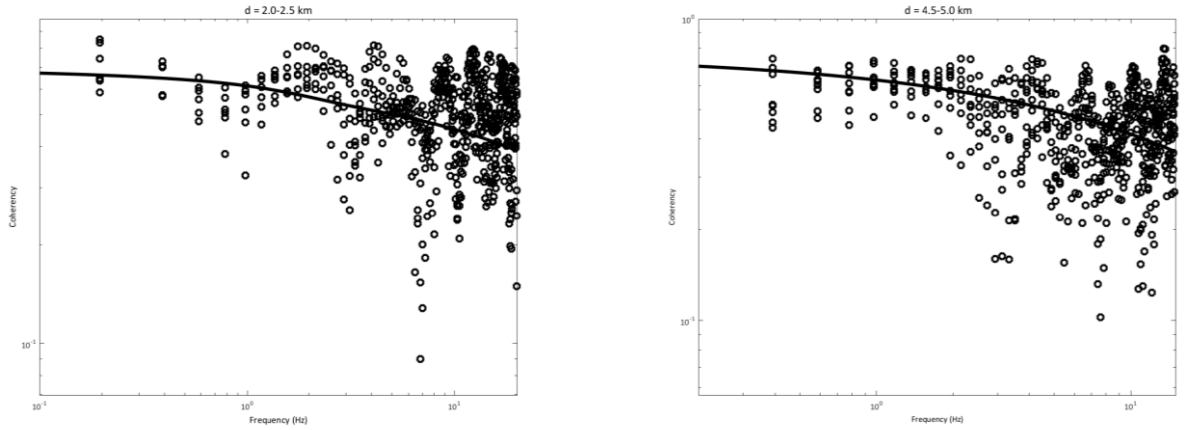

Figure 7. Comparison of coherency model with respect to observed coherency values for distance bins: (a) d=2.0-2.5 km, (b) d=4.5-5.0 km

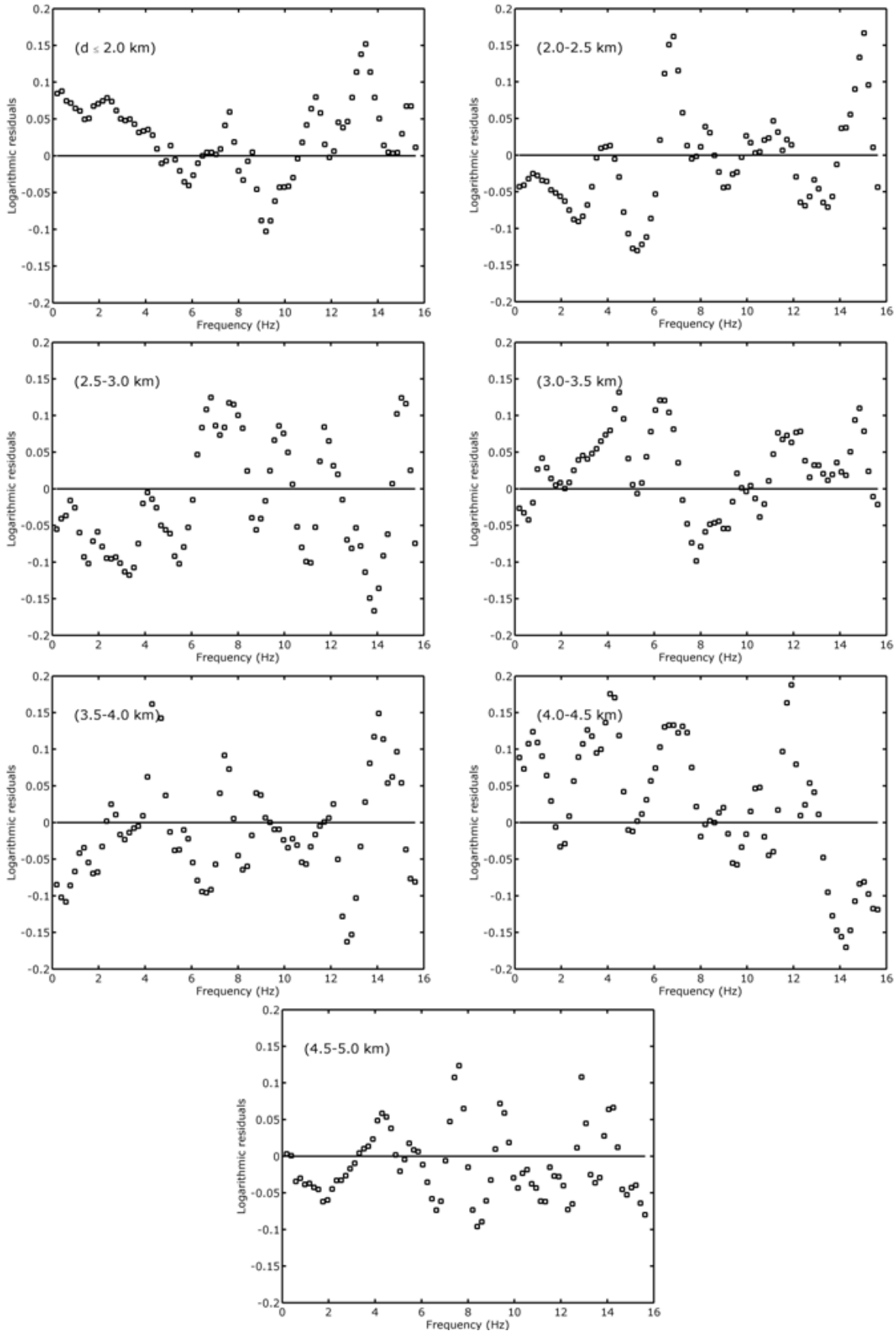

Figure 8. Residuals of the coherency model (Eq. 6) for each distance bin

the target coherency function. First, earthquake ground motion data compatible with design response spectrum are generated by code RSPMATCH2005 [53, 54]. Then, the ground motion data is simulated following Shama [34] to produce coherencies in agreement with the target coherency function.

Shama [34] assumed that the spatial variation of ground motion is the combined result of wave scattering and wave passage effects. A coherency model is used in which the wave scattering effects on the simulated ground motion is accounted for by the coherency phase $\mu_{i,j}$ and the wave travel effect is taken care of by the time lag between two stations as:

$$a(t) = \sqrt{2}\sum_{i=1}^{N_f}\sqrt{S_g(w_i)\,\Delta w}\cos\left[w_i(t - t_j) + j_i + m_{i,j}\right] \tag{7}$$

in which a(t) is the estimated ground motion acceleration; $S_g(\omega_i)$ is power spectrum of the initial motion; $\Delta\omega = \omega_u / N_f$, with ω_u as the cut-off frequency; τ_j represents the time lag between the two stations as $\tau_j = d_j / V$, where d_j is the separation distance between two stations; V is the apparent seismic wave velocity; $\emptyset_i$ represents the phase angle and N_f is number of frequency intervals.

The coherency phase $\mu_{i,j}$ for the i^{th} frequency at station j in Eq. 7 is stated as

$$m_{i,j} = \cos^{-1}\left[g(d_j, w_i)\; b\left(j_i, \frac{w_i d_j}{V}\right)\right] \tag{8}$$

where $\gamma(d_j, \omega_i)$ is the coherency model defined in Eq. 6 and written again as

$$|g(d,f)| = 0.513e^{(0.0781 - 0.038\sqrt{d})0.01f} + (1 - 0.513)e^{(-0.2643 - 0.0301d^2)(0.01f)^2} \tag{9}$$

where d is the separation distance between two stations and f is the frequency.

β is a function related to the coherency phase angle [34] and is defined as:

$$b = \{+1 \quad 0 < j \le 2p \qquad \text{for } \frac{wd}{V} \le 0.8 \tag{10a}$$

$$b = \begin{cases} -1 & 0 < j \le \frac{p}{2} \\ +1 & \frac{p}{2} < j \le p \\ -1 & p < j \le \frac{3p}{2} \\ +1 & \frac{3p}{2} < j \le 2p \end{cases} \qquad \text{for } 0.8 \le \frac{wd}{V} \le 2.5 \tag{10b}$$

$$b = \begin{cases} -1 & 0 < j \le \frac{p}{2} \\ \frac{p}{m} - 1 & \frac{p}{2} < j \le p \\ \frac{p}{m} + 1 & p < j \le \frac{3p}{2} \\ \frac{2p}{m} - 1 & \frac{3p}{2} < j \le 2p \end{cases} \qquad \text{for } \frac{wd}{V} > 2.5 \tag{10c}$$

where V is the apparent wave velocity.

Numerical Application

The numerical procedure explained above is applied to simulate ground motion at two locations with a relatively small separation distance for two example cases. In the first case, we select two stations, set 1.82 km apart, from the IERRS. We simulate acceleration recorded at one of them during a real earthquake with the help of recording at the other station and compare the results. We use an earthquake that is not included in the development of the coherency model for Istanbul. In the second case, we carry out a blind simulation. We select a recording of the 1999 Kocaeli earthquake. Using this record, we estimate ground motion 500 m away from the station, acknowledging the fact that the magnitude of the earthquake we simulate for, is beyond the magnitude range, for which we have developed our coherency model.

Briefly, the spectrum compatible time histories that have coherency values consistent with the prescribed coherency function are used to generate earthquake ground motion. The spectrum compatible acceleration is subdivided into time windows. The target power spectrum of each time window is formed by an autoregressive (AR) model. In this approach, ground motion is idealized by using a stochastic

harmonic model. A coherency model, which decreases exponentially, is used to represent the statistical dependence of the ground motion at another station [34].

This coherency model described in the previous section and expressed in Eq. 9 was employed as the coherency phase stated in Eq. 8. The computed power spectra, phase spectra, and coherency phase are used to generate the coherency model compatible with the earthquake ground motion (Eq. 7).

Results and Discussion

As the first example, the methodology is used to simulate an acceleration time history at station R85 of the IERRS. The distance from the record at station R00 (reference station) 1.82 km. The earthquake data obtained during the October 3, 2010 earthquake with a local magnitude of 4.4 is used. The reference acceleration ground motion data is shown at the top row in Figure 10a. As compared in Figure 10, the estimated ground motion data, at 1.82 km are compatible with those of the observed record. Furthermore, generated acceleration, ground velocity and displacement time histories are consistent with observed ground motion. Besides the fact that the Fourier amplitude spectrum of estimated ground motion data is in good agreement with the observed data at 1.82 km in the range of less than 10 Hz (Fig. 10d). As shown in Figure 10e, the acceleration response spectrum of the simulated motion slightly underestimates the observed response spectrum for low periods. On the contrary, the compatibility is good for the higher periods.

The target coherency spectrum (Eq. 9) at 1.82 km separation distance is plotted in Figure 10f. The coherency values calculated from simulated data are compared with the target coherency model. As shown in Figure 10f, the computed coherency values are consistent with that of the target coherency model.

As the second example, the procedure is applied to simulate an accelerogram at a distance of 500 m from the original record taken from MSK station of the August 17, 1999 Kocaeli earthquake (Mw 7.5). The hypo-central distance of the MSK station is 92.14 km. The sampling frequency of recorded ground motion is 200 Hz. The initial reference time history is shown in Figure 11a. This time history is modified to obtain the ground motion that is consistent with the target spectrum demonstrated in Figure 11c using RspMatch2005 software. It is seen that the five per cent damped response spectra for the simulated ground motion appear to be in good agreement with the target spectrum. The generated time histories compatible with prescribed target spectrum are displayed in Figure 11b. The results are consistent with the initial time histories shown in Figure 11a.

The acceleration time history demonstrated in Figure 11b is subdivided into windows with a power of 2 in length.

Acceleration, velocity, and displacement time histories of the initial reference station are compared with the acceleration, velocity, and displacement time histories at a distance of 500 m from the reference point. It is observed that the simulated time histories shown at the left column in Figure 12; conforms to the reference record. The differences between the simulated and initial ground motion, named as relative time history, are displayed at the right column in Figure 12a for acceleration; in Figure 12b for velocity; and in Figure 12c for displacement.

The frequency contents of the simulated data to that of reference data are compared. The Fourier amplitude spectra of the simulated and reference accelerations are plotted at the left hand side of Figure 13. The Fourier amplitudes of the reference data are compatible with those of the simulated motion. The target spectrum and the matched spectrum computed as a result of generation of target response spectrum compatible ground motion in Figure 11c are compared with spectral amplitudes of simulated data at the right column of Figure 13.

It can be argued that simulation of an earthquake of magnitude 7.2, using a coherency model developed for the magnitude range of 3.1 to 5.2, would lead to underestimation of ground motion for frequencies less than about 3 Hz. However, considering the Fourier amplitudes and response spectra of actual and simulated ground motion (Figure 13) does not suggest any significant deviation.

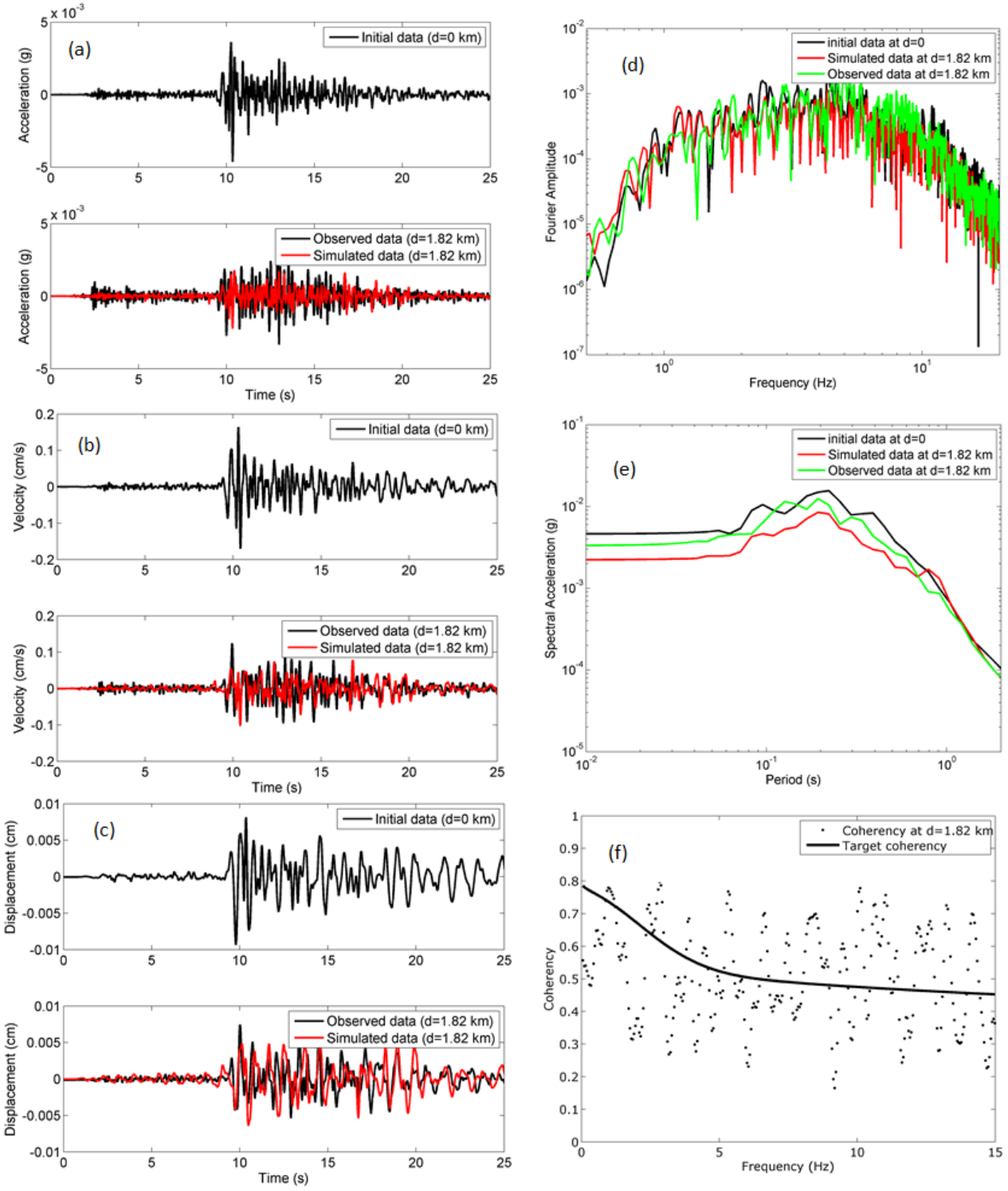

Figure 10. Comparison of observed and simulated acceleration data at d=1.82 km: (a) Acceleration time histories, (b) Velocity time histories, (c) Displacement time histories, (d) Fourier amplitude spectra, (e) Response spectra, (f) Coherency spectra

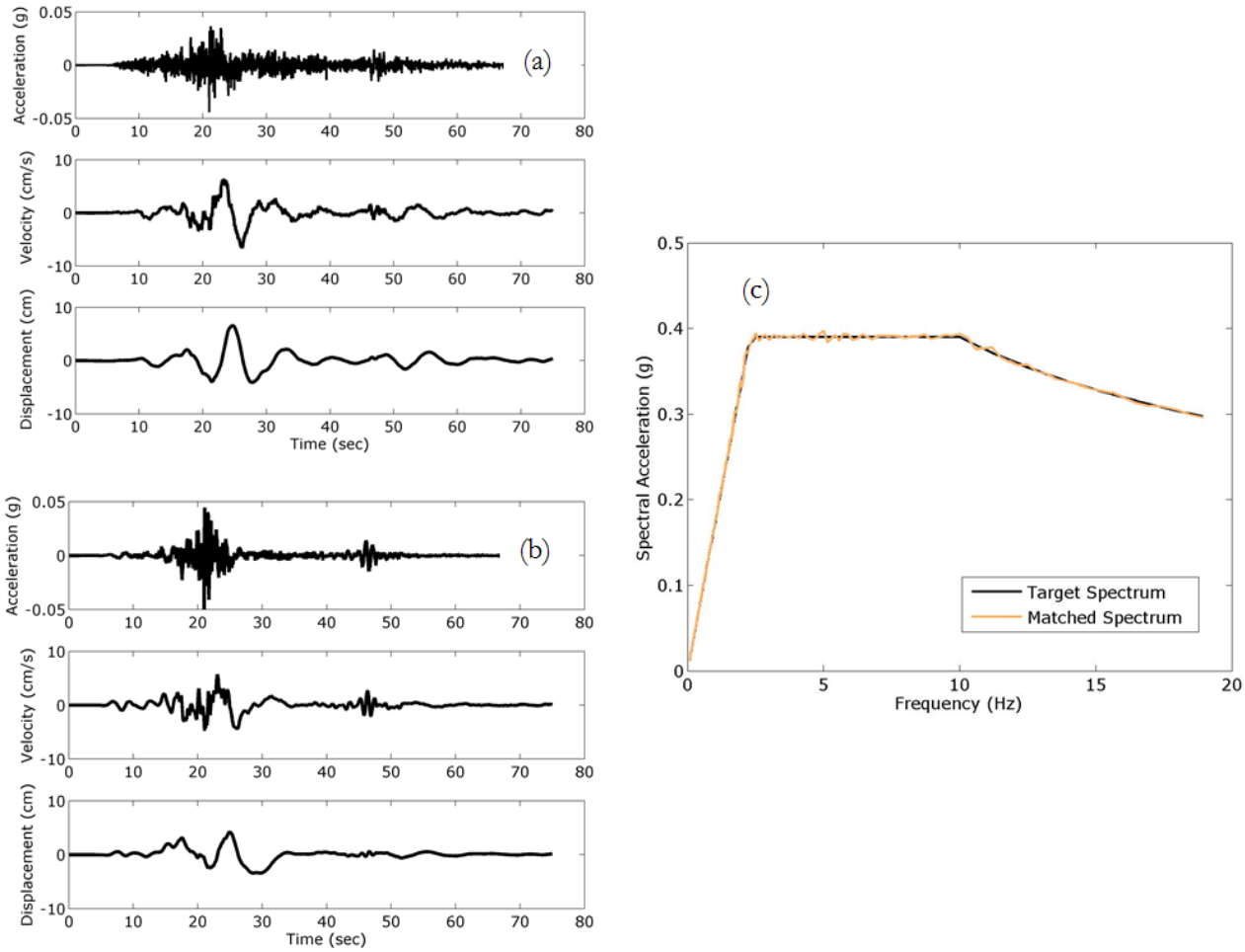

Figure 11. (a) The August 17, 1999 Kocaeli earthquake recorded at MSK station: Acceleration (g), velocity (cm/s) and displacement (cm); (b) Target spectrum compatible time histories: Acceleration (g), velocity (cm/s) and displacement (cm); (c) Comparison of target spectrum and the matched response spectrum

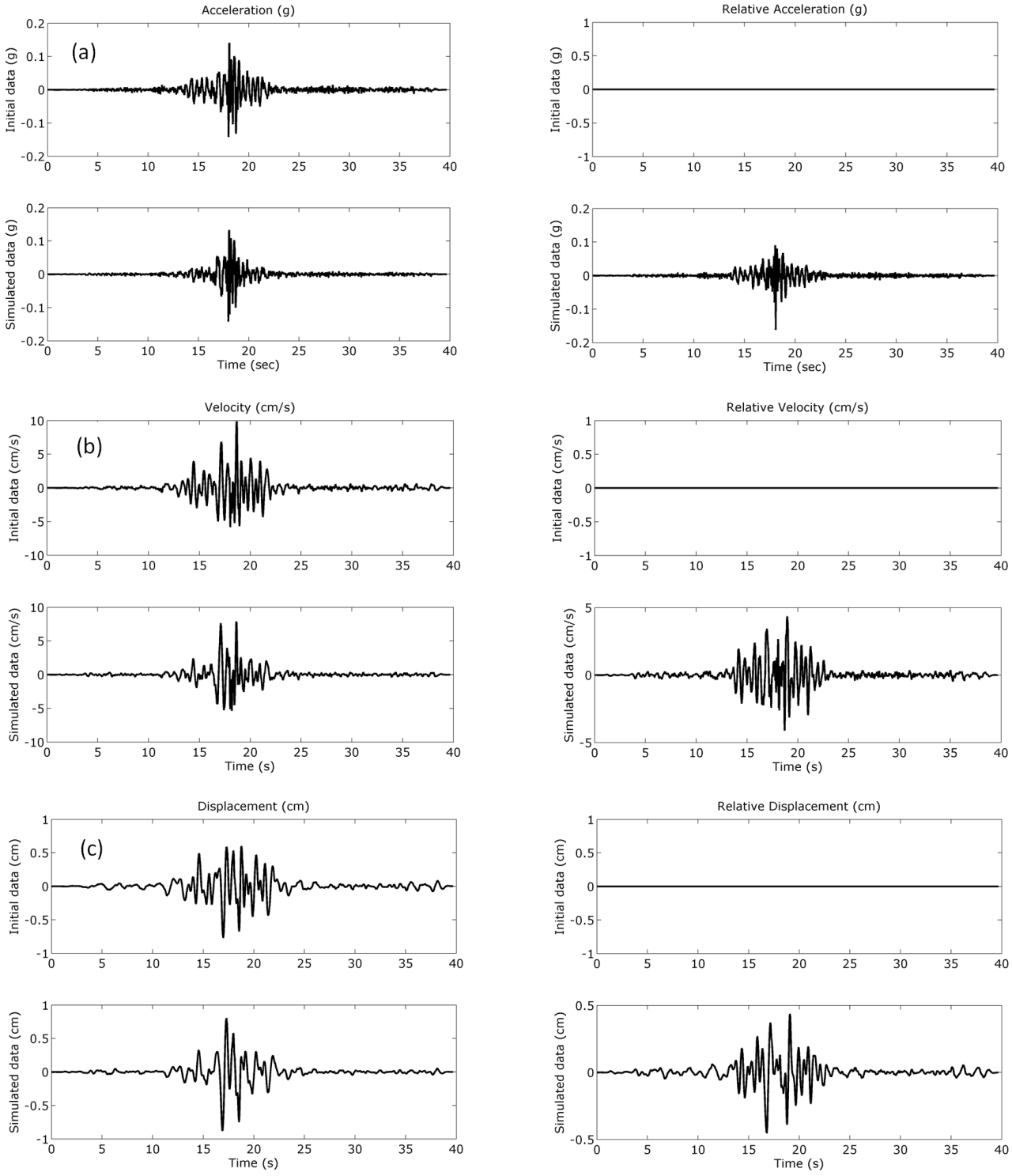

Figure 12. Acceleration (a), velocity (b) and displacement (c) time history of reference station and simulated data at d=500 m (left); relative related time history with respect to reference station (right)

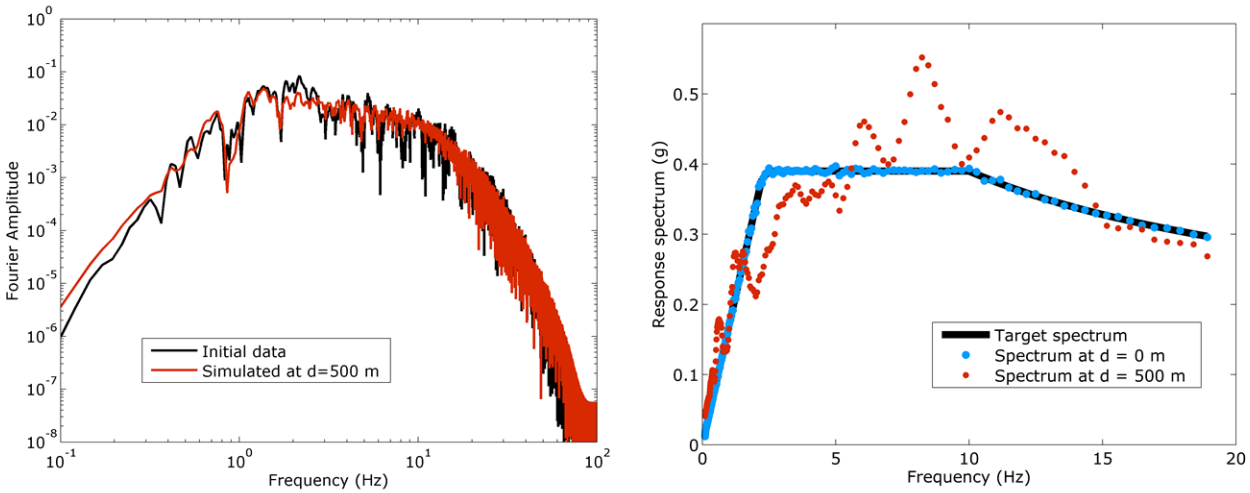

Figure 13. Comparison of Fourier amplitude of reference station and simulated data at d=500 m (left); comparison of target, spectrum at reference station and spectrum at d=500 m (right)

Conclusions

The design of extended structures such as bridges, pipelines should preferably be done considering the spatial variability of earthquake ground motion. In this context, frequency content of recorded earthquake ground motion data is used to obtain this variability.

In this paper, a coherency function for Istanbul is proposed. It is valid for the magnitude range of 3.1 to 5.2 and separation distances of up to 5 km. The proposed empirical coherency function considering frequency and separation distance is consistent with the observed data triggered by IERRS. The model can be utilized for the estimation of spatially variable earthquake ground motion in Istanbul. Then, the ground motion data is simulated following Shama [34] to produce coherencies in agreement with the target coherency function.

Secondly, the coherency values consistent with the prescribed coherency function are used for the spectrum compatible time histories, and then earthquake ground motion are generated using these values. For the validation of procedure, two separation distances, 0.5km and 1.82km are utilized. The simulated and reference acceleration ground motion data are in good agreement for both cases. Furthermore, velocity and displacement time histories are also compatible with observed data.

State-o-the-art studies show that simulation of the spatially correlated earthquake ground motion data for use in dynamic analysis of extended structures, tunnels, nuclear power plants (Liu and Hongs [55], Chen et al. [56], Ahmed et al. [57], Papadopoulos et al. [58], Wu et al. [59]).

In this context, this study forms the skeleton to simulate the ground motion consistent with the response and coherency characteristics of a region at stations distributed over an extended area.

References

1. Schneider, J.F.; Abrahamson, N.A.; Somerville, P.G.; Stepp, J.C. Spatial Variability of Ground Motion from EPRI's Dense Acceleragraph Array at Parkfield, California. *Proc Fourth U. S. National Conf Earthq Eng*, EERI, Palm Springs, 375-384, 1990.
2. Abrahamson, N.A.; Sykora, D. Variations of Ground Motions Across Individual Sites. *Proc Fourth DOE Natl Phenom Hazards Mitig Conf*, 9192-9198, Atlanta, Georgia, 1993.
3. Joyner, W.B.; Boore, D.M. Peak Horizontal Acceleration and Velocity from Strong-Motion Records Including Records from the 1979 Imperial Valley, California, Earthquake. *Bull Seism Soc Am* **1981**, *71*, 2011-2038.
4. Abrahamson, N.A. Statistical Properties of Peak Ground Accelerations Recorded by the Smart 1 Array. *Bull Seismol Soc Am* **1988,** *78*, 26-41.
5. Kawakami, H.; Mogi, H. Analyzing Spatial Intraevent Variability of Peak Ground Accelerations as a Function of Separation Distance. *Bull Seism Soc Am* **2003**, *93*, 1079-1090.
6. Field, H.E.; Hough, S.E. The Variability of PSV Response Spectra across a Dense Array Developed During the Northridge Aftershock Sequence. *Earthq Spectra* **1997**, *13*, 243-257.
7. Evans, J.R.; Hamstra, R.H.; Spudich, Jr.P.; Kündig , C.; Camina, P.; Rogers, J.A. TREMOR: A Wireless, MEMS Accelerograph for Dense Arrays. U.S.G.S. *Open File Repor*t **2003**, 03-159.
8. Loh, C.H. Analysis of the Spatial Variation of Seismic Waves and Ground Movements from SMART-1 Array Data. *Earthq Eng Struct Dyn* **1985**, *13*, 561–581.
9. McLaughlin, K.L. Spatial Coherency of Seismic Waveforms, PhD Thesis, University of California, Berkeley, 1983.
10. Abrahamson, N.A. Estimation of Seismic Wave Coherency and Rupture Velocity Using the SMART-1 Strong Motion Array Recordings. EERC *Report No. EERC/UCB/85-02* 1985, Earthquake Engineering Research Center, University of California.
11. Abrahamson, N.A. Spatial Variation of Multiple Support Inputs. *Proc the First U.S. Semin Seism Eval Retrofit Steel Bridges*, San Francisco, 1993.
12. Harichandran, R.S; Vanmarcke, E. Stochastic Variation of Earthquake Ground Motion in Space and Time. *J Eng Mech ASCE* **1986,** *112*, 154-174.
13. Harichandran, R.S. Local Spatial Variation of Earthquake Ground Motion. In *Earthquake Engineering and Soil Dynamics II - Recent Advances in Ground-Motion Evaluation*; Von Thun, J. L. (editor),. American Society of Civil Engineers, New York, 1988; pp. 203-217.

14. Harichandran, R.S. Estimating the Spatial Variation of Earthquake Ground Motion from Dense Array Recordings. *Struct Saf* **1991**, *10*, 219-233.
15. Loh, C.H.; Yeh, Y.T. Spatial Variation and Stochastic Modeling of Seismic Differential Ground Movement. *Earthq Eng Struct Dyn* **1988**, *16*, 583–596.
16. Loh, C.H.; Lin, S.G. Directionality and Simulation in Spatial Variation of Seismic Waves. *Eng Structs* **1990**, *12*, 134–143.
17. Novak, M. Discussion on Stochastic Variation of Earthquake Ground Motion in Space and Time by R. S. Harichandran and E. H. Vanmarcke. *J Eng Mech Div* **1987**, *113*, 1267–1270.
18. Oliveira, C.S.; Hao, H.; Penzien, J. Ground Motion Modeling for Multiple-Input Structural Analysis. *Struct Saf* **1991**, 10, 79–93.
19. Ramadan, O.; Novak, M. Coherency Functions for Spatially Correlated Seismic Ground Motions. *Geotechnical Research Center Report No. GEOT-9-93*, 1993;University of Western Ontario, London, Canada.
20. Vernon, F.; Fletcher, J.; Carroll Chave, A.; Sembera, E. Coherence of Seismic Body Waves as Measured by a Small Aperture Array. *J Geophys Res* **1991**, *96*, 11981–11996.
21. Zerva, A.; Zhang, O. Correlation Patterns in Characteristics of Spatially Variable Seismic Ground Motions. *Earthq Eng Struct Dyn* **1997**, *26*, 19–39.
22. Cacciola, P.; Deodatis, G. A method for generating fully non-stationary and spectrum-compatible ground motion vector processes. *Soil Dyn Earthq Eng* **2011**, *31*, 351-360.
23. Zerva, A.; Zervas, V. Spatial Variation of Seismic Ground Motions: An Overview. *Appl Mech Rev* **2002**, *55*, (3): 271-297.
24. Zerva, A. Spatial Variation of Seismic Ground Motions. CRS Press, New York: 2009.
25. Song, S.G.; Pitarka, A.; Somerville, P. Exploring Spatial Coherence between Earthquake Source Parameters. *Bull Seism Soc Am* **2009**, *99* (4): 2564-2571.
26. Harmandar, E.; Durukal, E.,; Erdik, M.; Özel, O. Spatial Variation Strong Ground Motion in Istanbul: Preliminary Results based on Data from the Istanbul Earthquake Rapid Response System. *European Geosciences Union (EGU) General Assembly*, Vienna, Austria, 2006.
27. Harmandar, E.; Durukal, E.; Erdik, M.; Ozel, O. Spatial Variation of Strong Ground Motion in Istanbul. *First European Conf Earthq Eng Seism*, Geneva, 2006.
28. Harmandar, E.; Durukal, E.; Erdik, M. A method for spatial estimation of peak ground acceleration in dense arrays. *Geophys J Int* **2012**, *191*, 1272–1284.
29. Rice, S.O. Mathematical Analysis of Random Noise. *Bell Syst Technical J* **1944**, *23*, 282–332.
30. Shinozuka, M. Monte Carlo Solution of Structural Dynamics. *Computers and Structs* **1972**, *2*, 855–874.
31. Conte, J.P.; Pister, K.S.; Mahin, S.A. Non-Stationary ARMA Modeling of Seismic Ground Motions. *Soil Dyn Earthq Eng* **1992**, *11*, 411-426.
32. Ellis, G.W.; Cakmak, A.S. Time Series Modeling of Strong Ground Motion from Multiple Event Earthquakes. *Soil Dyn Earthq Eng* **1991**, *10*, 42-54.
33. Mignolet, M.P.; Spanos, P.D. Simulation of Homogeneous Two-Dimensional Random Fields: Part I—AR and ARMA Models. *J Appl Mech* **1992**, *59*, 260–269.
34. Shama, A. Simplified Procedure for Simulating Spatially Correlated Earthquake Ground Motions. *Eng Structs* **2007**, *29*, 248-258.
35. Fenton, G.A.; Vanmarcke, E.H. Simulations of Random Fields via Local Average Subdivision. *J Eng Mech* **1990**, 116, 1733-1749.
36. Hao, H.; Oliveira, C.S.; Penzien, J. Multiple-Station Ground Motion Processing and Simulation based on SMART-1 Array Data. *Nuclear Eng Des* **1989**, *111*, 293-310.
37. Zerva, A,; Katafygiotis, L.S. Selection of Simulation Scheme for the Nonlinear Seismic Response of Spatial Structures. *Proc Fourth Int Colloq Computation of Shell and Spatial Structs*, Chania, Greece, 2000.
38. Abrahamson, N.A. Generation of Spatially Incoherent Strong Motion Time Histories. *Proc Tenth World Conf Earthq Eng*, Madrid, Spain, 1992.
39. Ramadan, O.; Novak, M. Simulation of Multidimensional Anisotropic Ground Motions. *J Eng Mechs* **1994**, *120*, 1773–1785.
40. Yamamoto, Y. Stochastic model for earthquake ground motion using wavelet packets. PhD Thesis, Stanford University, 2011.
41. Mirrashid, M.; Givehchi, M.; Miri, M,; Madandoust, R. Performance investigation of neuro-fuzzy system for earthquake prediction. *Asian J Civ Eng (BHRC)* **2016**, *17*, 213–223.
42. Matsushima, Y. Stochastic Response of Structure due to Spatially Variant Earthquake Excitations. *Proc Sixth World Conf Earthq Eng*, Vol. II, 1077-1082, Sarita Prakashan, Meerut, India, 1977.
43. Abrahamson, N.A.; Schneider, JF, and Stepp C. Spatial Variation of Strong Ground Motion for Use in Soil-Structure Interaction Analyses. Proc Fourth

U.S. Natl Conf Earthq Eng, Palm Springs, California, 1990.
44. Abrahamson, N.A.; Schneider, J.F.; Stepp; J.C. Empirical Spatial Coherency Functions for Applications to Soil-Structure Interaction Analyses. *Earthq Spectra* **1991**, *7*, 1-27.
45. Erdik, M.; Fahjan, Y.; Ozel, O.; Alcik, H.; Mert, A.; Gul, M. Istanbul Earthquake Rapid Response and the Early Warning System. *Bull Earthq Eng* **2003**, *1*, 157-163.
46. Boissieres, H.P.; Vanmarcke, E.H. Estimation of Lags for a Seismograph Array: Wave Propagation and Composite Correlation. *Soil Dyn Earthq Eng* **1995**, *14*, 5-22.
47. Parolai, S.; Ansal, A.; Kurtulus, A.; Strollo, A.; Wang, R.; Zschau, J. The Ataköy vertical array (Turkey): Insights into seismic wave propagation in the shallow-most crustal layers by waveform deconvolution. *Geophysical Journal International* **2009**, *178*, 3, 1649–1662. https://doi.org/10.1111/j.1365-246X.2009.04257.x.
48. Bolt, B.A.; Tsai Y.B.; Yeh. K.; Hsu, M.K. Earthquake strong ground motion recorded by a large near-source array of digital seismographs. *Earthq Eng Struct Dyn* **1982**, *10*, 561-573.
49. Porter, K.A. An Overview of PEER's Performance-based Earthquake Engineering Methodology. Proc Ninth Intern Conf Appls Stat Probab Civil Eng, San Francisco, California, 2003.
50. Songtao, L. Physical Characterization of Seismic Ground Motion Spatial Variation and Conditional Simulation for Performance-Based Design. PhD Thesis, Drexel University, 2006.
51. Das, S.; Gupta, V.K. Wavelet-Based Simulation of Spectrum-Compatible Aftershock Accelerograms. *Earthq Eng Struct Dyn* **2008**, *37*, 1333-1348.
52. Bi, K.; Hao, H. Simulation of Spatially Varying Ground Motions with Non-Uniform Intensities and Frequency Content. Earthq Eng Aust Conf, Ballarat, Australia, 2003.
53. Abrahamson, N.A. Non-stationary spectral matching program RSPMATCH. Pacific Gas and Electric Company Internal Report, 1998.
54. Hancock, J.; Watson-Lamprey, J.; Abrahamson, N.A.; Bommer, J.J.; Markatis, A.; McCoy, E.; Mendis, E. An improved method of matching response spectra of recorded earthquake ground motion using wavelets. *J Earthq Eng* **2006**, *10*, Special Issue I, 67-89.
55. Liu, T.J.; Hong, H.P. Application of spatially correlated and coherent records of scenario event to estimate seismic loss of a portfolio of buildings. *Earthq Spectra* **2015**, 31.4: 2047-2068.
56. Chen, Z.; Liang, S.; He, C. Effects of different coherency models on utility tunnel through shaking table test. *J Earthq Eng* **2020**, 24.4: 579-600.
57. Ahmed, K.; Kim, D.; Lee, S.H. Effect of the incoherent earthquake motion on responses of seismically isolated nuclear power plant structure. *Earthq Struc* **2018**, 14.1: 33-44.
58. Papadopoulos, S.; Sextos, A.; Know, O.; Gerasimidis, S.; Deodatis, G. Impact of spatial variability of earthquake ground motion on seismic demand to natural gas transmission pipelines. Proccedings of the 16th World Conference on Earthquake, 16WCEE, 2017.
59. Wu, Y.; Gao, Y.; Zhang, N.; Zhang, F. Simulation of spatially varying non-Gaussian and nonstationary seismic ground motions by the spectral representation method. *J Eng Mech* **2018**, 144.1: 04017143.